particles

MDPI

Article

A Systematic Approach to Studying Quark Energy Loss in Nuclei Using Positive Pions †

Nicolás Zambra-Gómez [1,2,*], William K. Brooks [1,3,*] and Nicolás Viaux [1,4,*]

[1] Departamento de Física, Universidad Técnica Federico Santa María, Casilla 110-V, Valparaíso 2340000, Chile
[2] Instituto de Física, Pontificia Universidad Católica de Valparaíso, Casilla 4059, Valparaíso 2362804, Chile
[3] Centro Científico Tecnológico de Valparaíso, Universidad Técnica Federico Santa María, Casilla 110-V, Valparaíso 2340000, Chile
[4] Millennium Institute for Subatomic Physics at High Energy Frontier (SAPHIR), Santiago 3871336, Chile
* Correspondence: nicolas.zambra@pucv.cl (N.Z.-G.); william.brooks@usm.cl (W.K.B.); nicolas.viaux@usm.cl (N.V.)
† This paper is based on the talk at the 13th International Conference on New Frontiers in Physics (ICNFP 2024), Crete, Greece, 26 August–4 September 2024.

Abstract: Our objective is to test the published models of partonic energy loss, particularly those describing the energy loss mechanisms of quarks traversing nuclear matter, within the framework of semi-inclusive deep inelastic scattering. Our methodological approach focuses on quantifying the quark energy loss in cold matter by analyzing the positive pions (π^+) produced in various nuclear targets, including deuterium, carbon, iron and lead, while our first approach only includes deuterium and carbon. Before normalizing the pions' energy distribution to unity to perform a shape analysis, acceptance corrections were performed to account for the detector's efficiency and ensure accurate comparisons of the spectra. By normalizing the energy spectra of π^+ produced from these distinct targets and based on the Baier–Dokshitzer–Mueller–Peigné–Schiff theory, which posits that quark energy loss depends only on nuclear size, it is assumed that the energy distributions of the targets will exhibit similar behavior. For this normalization, an energy shift between these distributions, corresponding to the quark energy loss, is identified. To ensure accuracy, statistical techniques such as the Kolmogorov–Smirnov test are used. The data used to test and explore the analysis technique and method were from the CLAS6 EG2 dataset collected using Jefferson Lab's CLAS detector.

Keywords: hadronization; semi-inclusive deep inelastic scattering; cold QCD matter; radiative energy loss

Academic Editors: Armen Sedrakian, Larissa Bravina and Sonia Kabana

Received: 31 December 2024
Revised: 12 February 2025
Accepted: 1 April 2025
Published: 15 April 2025

Citation: Zambra-Gómez, N.; Brooks, W.K.; Viaux, N. A Systematic Approach to Studying Quark Energy Loss in Nuclei Using Positive Pions. *Particles* **2025**, *8*, 44. https://doi.org/10.3390/particles8020044

1. Introduction: Hadronization

In deep inelastic scattering (DIS) [1], a high-energy incoming electron interacts with a valence quark in a nucleon through a virtual photon. If the energy transfer is sufficient, the quark is ejected from the nucleon. However, due to the principle of color confinement, the quark cannot exist in isolation in its colored state and must undergo hadronization, a transformation into a hadron, to remain color-neutral.

The experimental data analyzed in this study come from semi-inclusive deep inelastic scattering (SIDIS), where both the scattered electron and the resulting hadrons are measured, supporting an exploration of the hadronization dynamics.

The Lund String Model [2], developed at Lund University, is a theoretical framework for understanding hadronization. In this model, the quarks within a hadron are connected by a massless string of gluon field lines. As a quark moves apart from its partner, the

string stretches and stores energy. When the energy reaches a critical threshold, the string breaks, generating a new quark–antiquark pair. This model reflects the principles of asymptotic freedom and confinement inherent in quantum chromodynamics (QCD). The Lund String Model is incorporated into the PYTHIA event generator [3], a widely used tool for simulating hadronization in high-energy physics experiments.

Hadronization in a nuclear environment, as opposed to a vacuum, involves additional interactions due to the presence of partons in the medium. The EG2 experimental data analyzed in this work include nuclear targets such as carbon (C), iron (Fe), and lead (Pb), representing "cold QCD matter". As the quark traverses the nuclear medium while hadronizing, it may interact with other partons, leading to energy loss. Understanding this energy loss is the focal point of this study, as it impacts the final state of the hadrons observed and provides insight into hadronization processes within a nuclear medium.

1.1. The BDMPS-Z Model for Radiative Energy Loss

The Baier–Dokshitzer–Mueller–Peigné–Schiff–Zakharov (BDMPS-Z) [4] model describes the radiative component of the total energy loss experienced by high-energy partons traversing a medium. This model was independently developed using quantum field theory techniques by Baier et al. and through the path-integral formalism by Zakharov. Despite the differing approaches, both formalisms are equivalent and yield the same nuclear modification spectra.

As discussed extensively in [5], we focus on a heuristic interpretation of the radiative energy loss mechanisms. A key assumption of the model is that the scattering centers in the medium are static and uncorrelated. The energy loss per unit path length, $-\frac{dE}{dz}$, is calculated under the condition that hadronization occurs within the nuclear medium, i.e., $0 \leq \omega \leq E$. Under these assumptions, it has been demonstrated [4] that the energy loss follows two characteristic regimes:

- For short coherence lengths,

$$-\frac{dE}{dz} \approx \frac{\alpha_s}{\pi} N_c \frac{\mu^2}{\lambda} L. \tag{1}$$

- For large coherence lengths,

$$-\frac{dE}{dz} \approx \frac{\alpha_s}{\pi} N_c \frac{\mu^2}{\lambda} \sqrt{E}. \tag{2}$$

where coherence length refers to the spatial or temporal extent over which a gluon emission is coherent, meaning the emitted gluon remains influenced by interactions with the parton and the medium. These behaviors are illustrated schematically in Figure 1, highlighting the transition between regimes as a function of the medium's properties and path length. Further details are discussed in [4].

1.2. The Experimental Setup

1.2.1. The Continuous Electron Beam Accelerator Facility (CEBAF)

The data for this paper were obtained from the EG2 run period, conducted between 9 January and 5 March 2004, in Hall B at the Thomas Jefferson National Accelerator Facility (Jefferson Lab) in Newport News, Virginia, USA. Jefferson Lab is a national research facility managed by the United States Department of Energy and specializes in exploring the structure of nuclear matter. The facility is equipped with the CEBAF, a particle accelerator based on superconducting radiofrequency (SRF) technology, which provides continuous-wave electron beams for use in multiple experimental halls (Halls A, B, and C).

During the period of the EG2 experiment, the CEBAF operated with a maximum electron beam energy of 5.014 GeV. The CLAS (CEBAF Large Acceptance Spectrometer) [6]

detector in Hall B was employed for this work, designed to handle 5.014 GeV electron beams with a momentum resolution of 0.01% and a beam diameter ranging from 50 to 100 µm. By 2009, the CEBAF had begun to be upgraded to a 12 GeV electron beam capacity, with the enhanced accelerator able to recirculate a beam through two superconducting linacs up to four times before directing it to the experimental halls.

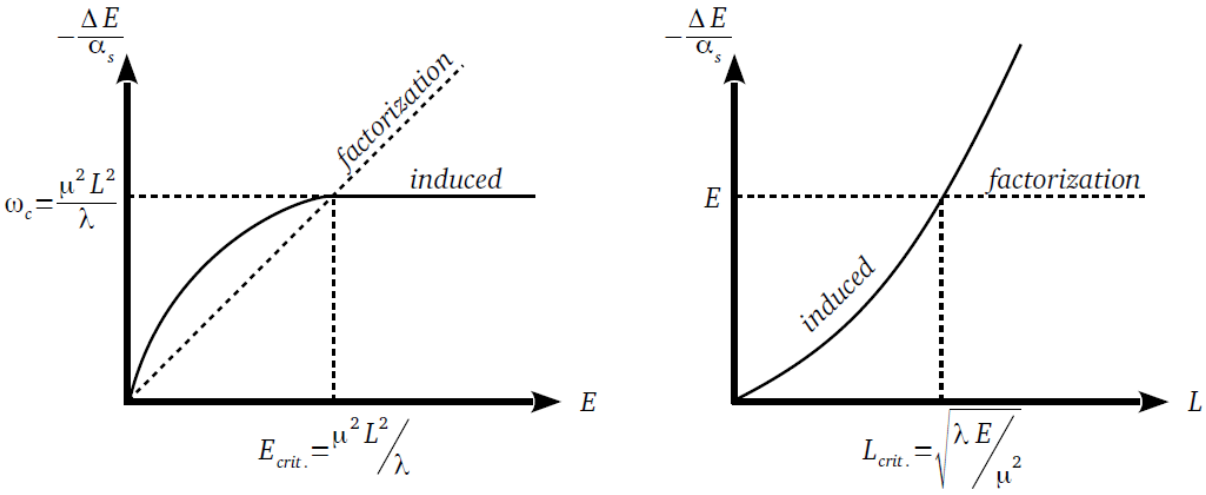

Figure 1. Illustration of the induced energy loss dependence on the parton energy E (**left**) and on the medium size L (**right**).

1.2.2. The CEBAF Large Acceptance Spectrometer (CLAS)

The CLAS detector [6] was the primary detector used in Hall B during the 6 GeV CEBAF era. This detector works well for studying multi particle final states, as it can detect charged particles and neutral particles. The detector consists of six identical sectors, with a schematic shown in Figure 2. The beam enters from the left side of the figure, with the target positioned near the center of the detector. The six superconducting coils surrounding the beam axis generate a toroidal magnetic field that is largely uniform in the azimuthal direction. This design allows for precise momentum and angle measurements for charged particles using a set of three drift chambers (DCs). Scintillator paddles provide time-of-flight (TOF) measurements, while a gas Cherenkov detector and an electromagnetic calorimeter aid in particle identification, particularly for electrons and pions.

Although it is primarily used for exclusive and semi-inclusive studies, as mentioned in [6], the CLAS detector can also handle inclusive electron scattering experiments. For the EG2c dataset, an open electron trigger was used, allowing for inclusive cross-section ratio measurements. During the EG2 experiment, both the Cherenkov detector and the electromagnetic calorimeter were included in the trigger, but their detection was limited to the forward direction, meaning that electrons could be detected at scattering angles of up to 55°. The detector's ability to maintain a near-zero magnetic field near the target also enables experiments with polarized targets, enhancing the momentum resolution and providing clear separation between the charged particle trajectories. The separation of the detector into six sectors by the toroidal magnetic field coils further helps manage the particle detection across its nearly 4π solid angle coverage.

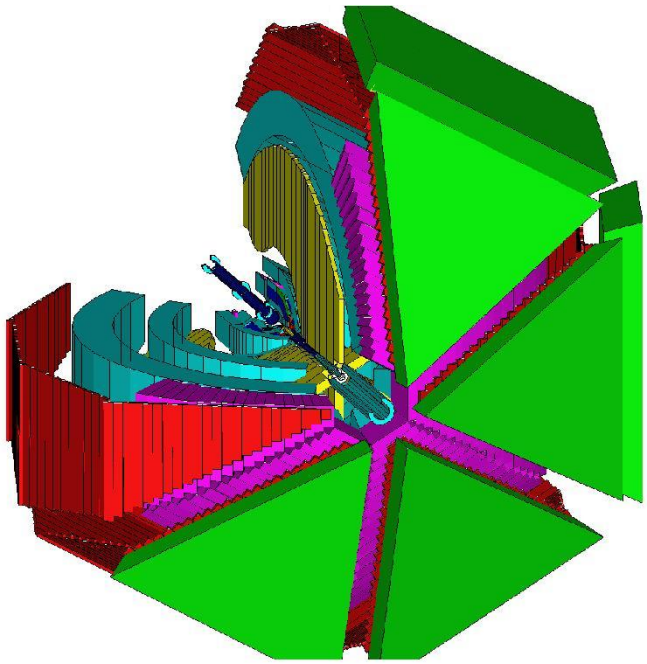

Figure 2. Green: Electromagnetic shower counters, Blue: Cherenkov counters, Red: Time-of-flight scintillators, Purple: Drift chambers regions, turquoise: Superconducting toroidal magnet. Note that there are regions where we have few or no events due to the limited detector acceptance [7].

1.3. Simulation

Simulations were crucial for addressing the limitations of the CLAS detector, such as the incomplete momentum space coverage and efficiency issues. They allowed us to model the behavior of the data before and after the interaction with the detector, ensuring reliable analysis results.

The simulations described in [8] involved two datasets: generated and reconstructed events. The generated events were created using PYTHIA 6.319, a Monte Carlo event generator that models both non-perturbative and perturbative DIS processes. Approximately 100 million events per nuclear target were produced as the basis for the dataset.

These "thrown" events were processed through GSIM, a GEANT 3-based simulation framework that models the CLAS's response. GSIM includes EG2-specific features, such as the energy loss and secondary particle radiation, implemented in [8].

The GSIM output was refined using the GSIM Post Processor (GPP), which accounted for detector imperfections, like malfunctioning drift chamber wires and scintillator issues. These data were then reconstructed using the RECSIS program, replicating the real data processing during the EG2 run.

2. Methodology

2.1. The Data Treatment

To ensure the quality and relevance of the data for analyzing the quark energy loss in different target types, a series of cuts were applied to the variables associated with the experiment (for definitions of these variables, the PDG's section on Structure Functions may be consulted). These cuts help isolate the desired physical processes and minimize background noise:

- Q^2: A cut is applied to the photon virtuality, restricting Q^2 to values between 1 and 4 GeV^2. This range helps ensure the interaction is in the deep inelastic scattering (DIS) regime, as well as avoiding energy dependency in terms of Q^2.

- W: Events with $W > 2$ GeV are selected to minimize the contributions of resonance, ensuring that we remain in the DIS region.
- x_B: The Bjorken scaling variable is restricted between 0.12 and 0.57, firstly to ensure that the scattering occurs on a single nucleon within the nucleus and avoids elastic scattering or processes where x_B exceeds unity and secondly to avoid energy dependency.
- y_B: A cut is applied to reduce radiative effects, which become increasingly significant at high values of y_B; a cut is applied such that $y_B < 0.85$.
- cut and target identification: After selecting electrons, pions, and DIS events, it is necessary to identify the target where the event occurred—either the solid or liquid target. Both targets are positioned along the z-axis, corresponding to the beam axis. A vertex cut is applied to the Z variable, which represents the vertex's position along the beam axis, to accurately distinguish between interactions in the liquid deuterium target and the solid targets. This cut ensures that events are correctly attributed to the target they originated from, minimizing contamination and enhancing the reliability of the analysis by focusing on interactions within the expected boundaries of each target type.

By implementing these cuts, we isolate events of interest to study the quark energy loss and minimize the effects of background noise and non-DIS contributions. Other cuts not mentioned here were applied following [9].

2.2. Modified Feynman-X

In semi-inclusive deep inelastic scattering (SIDIS) events, the final-state hadrons can originate from two main sources: the struck quark or the remaining target remnants. To distinguish these sources and analyze the hadronization process better, we introduce the Feynman-X (x_F) variable. The purpose of using x_F is to isolate hadrons produced primarily by the struck quark, minimizing the influence of the nuclear environment. To do so, we use a cut of $x_F > 0.1$. This cut reduces the contribution of the target fragments, emphasizing particles originating from the struck quark. However, this cut also leads to reduced statistics and potential mismatches at lower energy ranges due to the exclusion of low-energy hadrons.

In the laboratory frame, x_F is defined as

$$x_F = \frac{2\left[(\nu + m_p)\sqrt{P^2 - P_T^2} - \sqrt{Q^2 + \nu^2} \cdot Z_h \nu\right]}{(\nu + m_n)\sqrt{(W^2 - m_n^2 + m_{\pi^+}^2)^2 - 4W^2 \cdot m_{\pi^+}^2}} \tag{3}$$

where m_p, m_n, and m_{π^+} are the masses of the proton, neutron, and pion, respectively. Notice that x_F depends on the energy of the detected hadron.

Since our methodology involves manually introducing an energy shift ΔE (representing the quark energy loss) into the energy distribution, the x_F cut must be recalculated each time a shift is applied. The modified Feynman-X incorporating ΔE is given by

$$x_F = \frac{2\left[(\nu + m_p)\sqrt{(P + \Delta E)^2 - \left(1 + \frac{\Delta E}{P}\right)^2 P_T^2} - \sqrt{Q^2 + \nu^2} \cdot (Z_h \nu + \Delta E)\right]}{(\nu + m_n)\sqrt{(W^2 - m_n^2 + m_{\pi^+}^2)^2 - 4W^2 \cdot m_{\pi^+}^2}} \tag{4}$$

2.3. Coulomb Correction

In DIS experiments, a Coulomb correction is needed because the target nuclei's Coulomb field affects charged particles, especially at low energies (∼5 GeV). The produced field alters the momentum of incoming and scattered electrons and also impacts the π^+ particle. Here, we used the values obtained in [10], presented in Table 1.

Table 1. Estimation for Coulomb correction in different nuclear media.

Target	E (MeV)
^2D	0
^{12}C	2.9
^{56}Fe	9.4
^{208}Pb	20.3

2.4. Acceptance Correction

Applying a simulation factor to each bin in the experimental data corrects the inefficiencies of the detector. For the CLAS detector, acceptance combines geometric acceptance with the detector inefficiencies from the drift chambers, scintillator counters, track reconstruction, and event selection. We introduce the acceptance factor A:

$$A = \frac{N_{rec}}{N_{gen}} \tag{5}$$

where N_{rec}, N_{gen} are the number of entries for reconstructed and generated bins.

In the application of the acceptance correction factor, each individual bin is treated as an independent entity. Consequently, for every bin in this n-dimensional space, there must be a corresponding A factor. This means that the binning scheme used in the simulation to obtain the acceptance factors must be the same used in the experimental data. The data are corrected using a weight of $\omega = 1/A$.

To bin the data distribution and treat each bin as an independent entity, a set of independent variables that do not directly affect the energy distribution must be selected to fully characterize our topic. Once the independent variables are established, all of the other kinematic quantities can be derived. Therefore, the calculations of the energy distribution acceptance factors were conducted bin by bin. Considering the production of a single pion electron at a fixed beam energy as an event, we propose the binning scheme shown in Table 2, where Φ_{PQ} is defined as the angle between the leptonic plane and the hadronic plane.

Table 2. Binning scheme considering the independent variables Q^2, x_B for the outgoing electron and P_t^2, Φ_{PQ} for the positive pion.

Variables	Lower Value	Upper Value	Steps	Total Steps
Q^2	1.0	4.0	0.5	6
X_B	0.12	0.57	0.9	5
Φ_{PQ}	-180	180	30	12
P_T^2	0.0	1.0	0.2	5

2.5. Quark Energy Loss Measurements

This analysis focuses on the energy spectrum of pions from both solid and liquid targets to extract their quark energy loss E in nuclear media. Deuterium is used as a control, representing scatterings in which quarks propagate in a "vacuum". A comparison of the

energy spectrum for deuterium with that of solid targets (C, Fe, and Pb) reveals a horizontal shift due to the energy loss in nuclear matter, recognized as the quark energy loss.

To quantify this shift, incremental energy offsets dE are applied to the solid target spectra, creating "shifted distributions". A statistical test compares each shifted distribution with the deuterium spectrum, iteratively identifying the shift dE that maximizes the probability of the test, which implies that there is no remaining energy loss after the shift.

2.6. The Kolmogorov–Smirnov Test

The Kolmogorov–Smirnov (KS) test is employed to quantify this shift. This statistical method compares one-dimensional distributions by assessing the maximum distance between their empirical cumulative distribution functions. Specifically, the two-sample KS test is used here to evaluate the similarity between the energy spectrum of deuterium and those of the shifted solid target distributions. The goal is to find the shift dE that maximizes the probability of the test.

The KS test offers the advantage of being a robust non-parametric method sensitive to differences in both the location and shape between distributions. It does not rely on assumptions about the underlying distribution, making it suitable for this analysis. However, it performs best with continuous distributions and is more sensitive near the center of the distributions than at the tails. Despite these limitations, the exact nature and reliability of the KS test make it an effective tool for identifying the quark energy loss.

3. Systematic Uncertainties

In the present analysis, systematic uncertainties were evaluated to quantify the impact of our assumptions and methodological choices on the final results. A key source of systematic uncertainty arises from the granularity of the energy step size used in the Kolmogorov–Smirnov (KS) test. For this study, the energy interval per iteration was set to 1 MeV, ensuring manageable computational costs while maintaining a sufficient resolution to capture the variations in the nuclear spectra.

The choice of a 1 MeV step introduces potential biases into the estimation of the quark energy loss, as finer or coarser resolutions could alter the sensitivity of the KS test to subtle differences between the experimental and theoretical distributions. To estimate the corresponding systematic uncertainty, varying the step size allows for an evaluation of the magnitude of this systematic effect, for example, including steps of 0.1 MeV and 0.01 MeV.

Furthermore, the systematic uncertainty due to the energy step size propagates into the estimation of the total induced energy loss and its scaling with the medium size L and parton energy E. This uncertainty may be related to the KS test results across different step sizes in order to analyze their influence on the extracted scaling exponents and nuclear spectra parameters.

In addition to the energy step size, other sources of systematic uncertainty include corrections for Coulomb effects and acceptance in the experimental data.

4. Results

We focus only on the carbon target, with the final goal of applying it to the other nuclear targets in the experimental data. Our first proof of concept was carried out using carbon data acceptance-corrected only in ϕ_{PQ} (that is, only 1D in our binning scheme) using steps of 1 MeV, as shown in Table 3.

To qualitatively estimate the systematic uncertainties, we conducted additional analyses using finer energy steps of 0.1 MeV, as shown in Table 4.

Table 3. *P*-values from the KS test for 1D acceptance-corrected data in ϕ_{PQ} from carbon data in steps of 1 MeV.

Energy (MeV)	*p*-Value
10	0.0758063
11	0.0843248
12	0.0887374
13	0.0958581
14	0.0874126
15	0.082802
16	0.082802
17	0.0884609
18	0.0744281
19	0.0695403

Table 4. *P*-values from the KS test for 1D acceptance-corrected data in ϕ_{PQ} from carbon data in steps of 0.1 MeV.

Energy (MeV)	*p*-Value
12.1	0.0887374
12.2	0.101077
12.3	0.098438

From the results, the consistency of the *p*-values across both the 1 MeV and 0.1 MeV binning steps demonstrates the stability of the analysis method. The relatively uniform distribution of the *p*-values across finer bins further supports the robustness of the proposed approach, minimizing concerns about binning-related systematic effects.

Discussion

This work introduces a data analysis method that prioritizes the technique itself over the specific details of the CLAS dataset. By doing so, the approach sidesteps the challenges associated with the preliminary nature of the data and focuses instead on the consistency of the theoretical framework. This method demonstrates robust alignment with the BDMPS theory, reinforcing its principles even when faced with potential adjustments to the experimental data. The reliance on CLAS FORTRAN GEANT 3 simulations, a well-tested and widely accepted tool, further validates the robustness of this methodology.

It is worth mentioning that some of the data presented in the tables from the results in Section 4 should not exhibit such uniformity in principle. This is particularly noticeable for carbon, where the amount of quark energy loss is low compared to that for the other targets. Since this is a shape analysis, it is expected that a range of possible values would satisfy the criteria set by the KS test in this case. Although the complete analysis requires considering the entire proposed binning scheme, analyzing a single bin can provide valuable intuition about the behavior of the data.

Additionally, it is important to note that other energy values not included in the tables showed *p*-values below 0.08 and drastically dropped to 0 as the energy approached around 13 MeV. This trend highlights the sensitivity of the KS test to deviations in the shape of the distributions.

Another relevant point of discussion involves the definition of Feynman-X. While the prevalent approach in the community relies solely on electron variables, our method incorporates additional kinematic details to offer a broader perspective on fragmentation.

This alternative definition not only enhances the analysis but also invites new insights into partonic energy loss and hadronization processes.

5. Conclusions

We introduce a systematic way to study the quark energy loss in nuclear matter using positive pion (π^+) production data from SIDIS experiments. Using data from the EG2 experiment at Jefferson Lab, we explored the hadronization process in nuclear targets of varying sizes, such as deuterium, carbon, iron and lead. As a proof of concept, we first focus on a carbon target. The energy distribution of π^+ reveals a consistent energy shift attributed to the quark energy loss. This shift was quantitatively assessed using statistical methods, including the Kolmogorov–Smirnov test, ensuring robust and reliable comparisons. The use of acceptance corrections, Coulomb corrections, and target-specific vertex cuts ensured that the observed energy distributions were free from detector biases and accurately reflected the underlying physical processes.

Overall, this study demonstrates the utility of using the π^+ production in SIDIS to probe quark energy loss mechanisms. The findings highlight the importance of nuclear size as a variable in understanding hadronization in cold matter, with implications for both theoretical models and experimental methodologies.

Author Contributions: All the authors contribute equally to the article. All authors have read and agreed to the published version of the manuscript.

Funding: This work was funded by ANID PIA/APOYO AFB230003, Millennium Program—ICN2019_044.

Data Availability Statement: Data is unavailable due to privacy restrictions.

Acknowledgments: N.Z.-G. acknowledges the Doctoral scholarship of Pontificia Universidad Católica de Valparaíso, granted by the Graduate Studies Directorate.

Conflicts of Interest: The authors declare no conflicts of interest.

References

1. Langacker, P. *The Standard Model and Beyond*, 2nd ed.; Taylor & Francis Group, LLC.: Abingdon, UK, 2017.
2. Andersson, B.; Gustafson, G.; Ingelman, G.; Sjöstrand, T. Parton Fragmentation and String Dynamics. *Phys. Rep.* **1983**, *97*, 31–145. [CrossRef]
3. Sjöstrand, T.; Ask, S.; Christiansen, J.R.; Corke, R.; Desai, N.; Ilten, P.; Mrenna, S.; Prestel, S.; Rasmussen, C.O.; Skands, P.Z. An introduction to PYTHIA 8.2. *Comput. Phys. Commun.* **2015**, *191*, 159–177. [CrossRef]
4. Baier R.; Dokshitzer, Y.L.; Mueller, A.H.; Peigne, S.; Schiff, D. Radiative energy loss of high energy quarks and gluons in a finite volume quark-gluon plasma. *Nucl. Phys. B* **1996**, *483*, 291–320. [CrossRef]
5. Aravena O. Parton Energy Loss Estimates Using Positive Pions in DIS on Nuclear Targets (CLAS EG2-Experiment). Master's Thesis, Universidad Tecnica Federico Santa Maria, Valparaíso, Chile, 2017.
6. Mecking B.; Adams, G.; Ahmad, S.; Anciant, E.; Anghinolfi, M.; Asavapibhop, B.; Asryan, G.; Audit, G.; Auger, T.; Avakian, H.; et al. The CEBAF large acceptance spectrometer (CLAS). *Nucl. Instruments Methods Phys. Res. A* **2003**, *503*, 513–553. [CrossRef]
7. Carman, D.S.; Joo, K.; Mokeev, V.I. Strong QCD Insights from Excited Nucleon Structure Studies with CLAS and CLAS12. *Few Body Syst.* **2020**, *61*, 29. [CrossRef]
8. Hakobyan, H. Observation of Quark Propagation Pattern in Nuclear Medium. Ph.D. Thesis, Yerevan State University, Yerevan, Armenia, 2008.
9. Vásquez, S.M. Studying of Hadronization Process Using Positive Pions with CLAS in Jefferson Lab. Master's Thesis, Universidad Tecnica Federico Santa Maria, Valparaíso, Chile, 2021.
10. Schmookler, B. Nucleon Structure and Its Modification in Nuclei. Ph.D. Thesis, Massachusetts Institute of Technology, Cambridge, MA, USA, 2018.